

Prismatic analyser concept for neutron spectrometers

Jonas O. Birk, Márton Markó, Paul G. Freeman, Johan Jacobsen, Rasmus L. Hansen, Niels B. Christensen, Christof Niedermayer, Martin Månsson, Henrik M. Rønnow, and Kim Lefmann

Citation: [Review of Scientific Instruments](#) **85**, 113908 (2014); doi: 10.1063/1.4901160

View online: <http://dx.doi.org/10.1063/1.4901160>

View Table of Contents: <http://scitation.aip.org/content/aip/journal/rsi/85/11?ver=pdfcov>

Published by the [AIP Publishing](#)

Articles you may be interested in

[The new cold neutron chopper spectrometer at the Spallation Neutron Source: Design and performance](#)
Rev. Sci. Instrum. **82**, 085108 (2011); 10.1063/1.3626935

[Novel concept of time-of-flight neutron spectrometer for measurement of the D/T burning ratio in the ITER](#)
Rev. Sci. Instrum. **77**, 10E721 (2006); 10.1063/1.2352740

[The TOFOR neutron spectrometer and its first use at JET](#)
Rev. Sci. Instrum. **77**, 10E702 (2006); 10.1063/1.2219422

[Calibration of the MEDUSA neutron spectrometer \(abstract\)](#)
Rev. Sci. Instrum. **72**, 845 (2001); 10.1063/1.1323488

[A sensitive neutron spectrometer for the National Ignition Facility](#)
Rev. Sci. Instrum. **72**, 846 (2001); 10.1063/1.1323242



Prismatic analyser concept for neutron spectrometers

Jonas O. Birk,¹ Márton Markó,² Paul G. Freeman,³ Johan Jacobsen,¹ Rasmus L. Hansen,¹ Niels B. Christensen,⁴ Christof Niedermayer,² Martin Månsson,^{2,3} Henrik M. Rønnow,^{1,3} and Kim Lefmann¹

¹*Nano Science Center, Niels Bohr Institute, University of Copenhagen, DK-2100 Copenhagen Ø, Denmark*

²*Laboratory for Neutron Scattering and Imaging, Paul Scherrer Institute, CH-5232 Villigen PSI, Switzerland*

³*Laboratory for Quantum Magnetism, École Polytechnique Fédérale de Lausanne (EPFL), CH-1015 Lausanne, Switzerland*

⁴*Institute of Physics, Technical University of Denmark, DK-2800-Kgs. Lyngby, Denmark*

(Received 15 September 2014; accepted 26 October 2014; published online 26 November 2014)

Developments in modern neutron spectroscopy have led to typical sample sizes decreasing from few cm to several mm in diameter samples. We demonstrate how small samples together with the right choice of analyser and detector components makes distance collimation an important concept in crystal analyser spectrometers. We further show that this opens new possibilities where neutrons with different energies are reflected by the same analyser but counted in different detectors, thus improving both energy resolution and total count rate compared to conventional spectrometers. The technique can readily be combined with advanced focussing geometries and with multiplexing instrument designs. We present a combination of simulations and data showing three different energies simultaneously reflected from one analyser. Experiments were performed on a cold triple axis instrument and on a prototype inverse geometry Time-of-flight spectrometer installed at PSI, Switzerland, and shows excellent agreement with the predictions. Typical improvements will be 2.0 times finer resolution and a factor of 1.9 in flux gain compared to a focussing Rowland geometry, or of 3.3 times finer resolution and a factor of 2.4 in flux gain compared to a single flat analyser slab. © 2014 AIP Publishing LLC. [<http://dx.doi.org/10.1063/1.4901160>]

I. INTRODUCTION

Most crystal analyser neutron spectrometers such as triple axis spectrometers (TAS) rely on the analyser mosaicity to provide the desired compromise between intensity and energy resolution.¹ Coarse analyser mosaicity means reflection of a larger energy range resulting in higher recorded flux but coarse resolution, while fine mosaicity brings the opposite result. For cold neutron spectrometers the most common analyser material is Pyrolytic Graphite (PG), using the (002) reflection with typical mosaicities of 20'–40' ($\frac{1}{3}^\circ - \frac{2}{3}^\circ$) FWHM as seen, e.g., on TASP at PSI,² PANDA at FRM II,³ 4F1, 4F2 at LLB⁴ and SPINS at NIST.⁵ However as neutron spectroscopy moves towards smaller sample sizes, the natural collimation produced by the distance between, e.g., sample and analyser can become comparable to, or better than, the mosaicity of standard graphite analysers. It has been shown that relying on distance collimation instead of mosaicity and the conventional parallel beam approximation can lead to better performing monochromators⁶ so it would be natural if the same was true for analysers. We will show that this is indeed the case and additionally demonstrate the opportunity to analyse several energy bands simultaneously with a single analyser. First we will describe the geometric effects in scattering from a single analyser slab, and then move to more advanced focussing and multiplexed setups. Finally, we show how our ideas are verified by both experiments and simulations leading to simultaneous gains in flux and resolution.

II. INSTRUMENT AND SIMULATIONS

The concept discussed in this article was developed for the CAMEA inverse time-of-flight spectrometer proposed for the European Spallation Source (ESS).⁷ Although the ideas are applicable to many crystal analyser spectrometer designs, they will be discussed based on the 5 meV CAMEA analyser as this specific setup has been thoroughly investigated. The analyser is placed at $L_{SA} = 1.46$ m from the sample. It consists of five wafers with three analyser crystals each that are 1.0 cm wide, 5.0 cm long, and reflecting out of the horizontal scattering plane. Neutrons are recorded by several parallel ³He 1/2" (1.27 cm) linear position sensitive detector tubes at a distance $L_{AD} = 1.25$ m. The settings are optimised for sample heights up to $h_S = 1.0$ cm. All the work is done based on these settings unless stated otherwise. Monte Carlo ray-tracing simulations were performed using the McStas package.^{8,9}

III. ELEMENTS OF THE PRISMATIC ANALYSER CONCEPT

The prismatic analyser uses a combination of distance collimation and an auto focussing effect from the analysers to achieve its results. We will here describe these effects before explaining the prismatic analyser itself.

A. Distance collimation

Distance is used in neutron instrumentation as a supplement to collimators to achieve a well collimated beam.^{10–12}

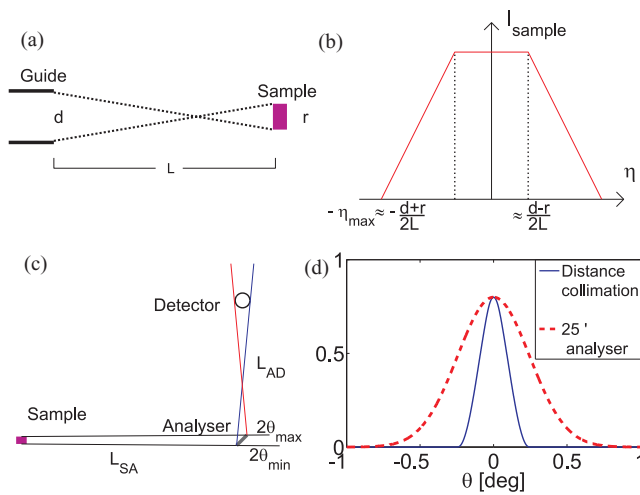


FIG. 1. Distance collimation. (a) Geometrical constraints limits the possible paths, e.g., from guide to sample. This will lead to a divergence distribution on the sample as shown in (b), assuming uniform divergence and position distributions with no correlations at the end of the guide. (c) The effect of distance collimation on analysers. Due to the geometrical restrictions only polychromatic scattering with a Bragg angle between $2\theta_{min}$ and $2\theta_{max}$ can reach the detector independently of the analyser mosaicity. The corresponding rays that cross between sample and analyser have less extreme angles when sample and detector are approximately equal in size and $L_{SA} > L_{AD}$. (d) Comparison of the resolution from distance collimation (numerically calculated) and a typical PG (002) analyser mosaicity (25') for the reference 5 meV CAMEA analyser.

If two parts of an instrument (for example, the guide end and the sample) have a maximum size and a certain distance between them then the maximal divergence that can propagate through the instrument is limited (see Figures 1(a) and 1(b)). We denote these geometrical constraints *distance collimation*. In our prismatic analyser setting we compute the correlated distance collimation contributions between sample and analyser and between analyser and detector. We therefore consider the maximum variation in Bragg angle that allows reflection from somewhere on the sample via any spot on the analyser to somewhere on the detector (see Figure 1(c)). For our reference setup this leads to a distance collimation (shown in Figure 1(d)) of the order 12' FWHM and thus dominates the mosaicities of most graphite analysers. This makes it possible to relax the mosaicity further with no change in energy resolution.

B. The auto-focus effect

A monochromatic neutron beam will be focused at a certain distance by a single, flat analyser slab. This “auto-focus” is illustrated in Figure 2. Panel (a) illustrates how a perfect monochromatic beam is reflected and focused by an analyser with a coarse mosaicity. Simulations of this effect using three narrow energy bands (c)–(e) confirm the effect by a clear narrowing of the reflected beam at 80–100 cm from the analyser. The exact focussing spot will move further away (and be more focussed) for smaller sample sizes, so it is not possible to define an exact focussing position for a general sample. However it is possible to construct the system so the auto focus point will be close to the detectors for a wide range of sample sizes.

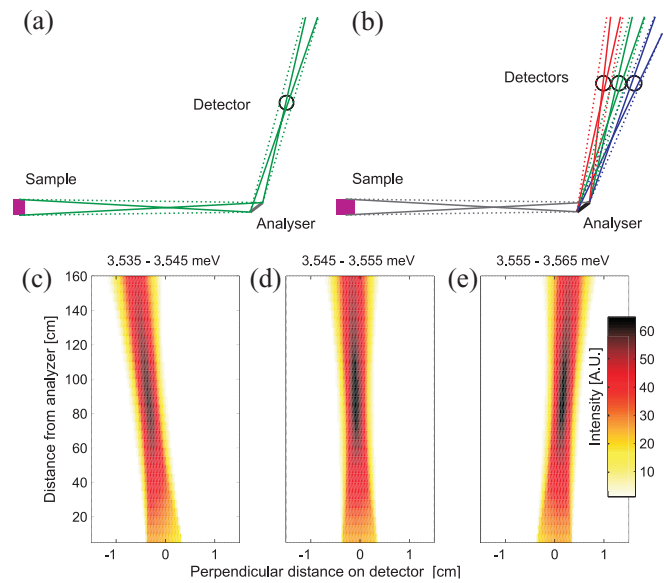


FIG. 2. (a) Reflection of a monochromatic beam from a single analyser crystal focussing at a certain distance. The solid and dashed lines represent the limits of the scattered rays. The outer gives the width of the beam while the inner illustrates how focused the beam will be. (b) Reflection of three specific energies (red, green, blue, respectively) from a single analyser crystal. Each energy is illustrated as in (a) and reflected in a specific angle given by Bragg’s law. The large difference in focussing distance is due to the exaggerated sample size, analyser size, and angular separation. (c)–(e) McStas simulation of the beam profile as a function of distance from the analyser of three adjacent energy bands, centered at 3.54 meV, 3.55 meV, and 3.56 meV from a single reflecting analyser piece. The horizontal scale has been expanded by a factor 20 for clarity. The autofocus is at 60–120 cm.

C. A single prismatic analyser

If distance collimation is the dominant part of the energy resolution, the analyser crystal will reflect a wider energy band than measured by the detector. Neutrons with other energies will be reflected at slightly different angles as described by Bragg’s law, and thus miss the detector. For example, the reference 5 meV analyser has a mosaicity of $60' = 1^\circ$ so the spread in scattering angle is 2° (FWHM) and the real space FWHM of the beam spot at the detector position is 4.4 cm, substantially larger than the 1.27 cm width of the detector tube. However, due to the distance collimation each specific energy will be reflected into a much smaller angular band. Figure 2 shows how three different monochromatic beams are reflected from the same analyser and recorded by three different detectors (b). McStas simulations of three narrow adjacent energy bands are shown in (c)–(e). Although there is some overlap it is clear that the energy affects the direction of the reflected beam. If a sufficient number of detectors are installed, the entire flux reflected from the analyser will be recorded. In addition, the improved distance collimation provides an accurate determination of the Bragg angle. This provides a better resolution than most mosaicity limited spectrometers together with comparable total count rates from the same analyser.

D. Simulated performance of the prismatic analyser

Figure 3 shows McStas simulations of reflected intensity and energy resolution for different analyser mosaicities.

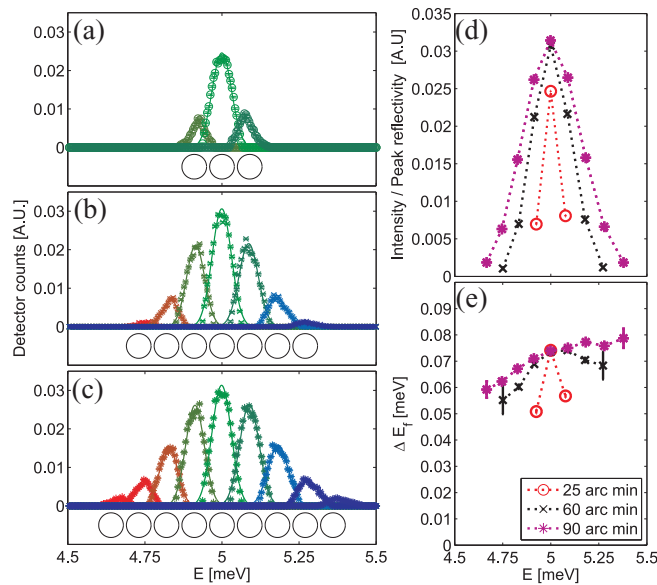


FIG. 3. Simulated recordings of several energies from a single analyser illuminated with a white beam. Each peak in (a)–(c) represents the counts in a single detector tube as function of E_i (the detector tubes are represented by circles below the data). The mosaicity of the analyser is $25'$ for (a), $60'$ for (b), and $90'$ for (c). (d) The corresponding intensities before correcting for peak reflectivity and (e) the energy resolution (FWHM) of the detectors for the three different mosaicity values.

We see that coarser analysers allow detection of more energies and will even detect slightly more neutrons in the central detector. However coarser graphite will in practice lower the peak reflectivity counteracting this gain. Peak reflectivity depends on analyser thickness, manufacturing process and the reflected energy^{13,14} and can only be applied to the results once these parameters are determined. The resolution broadens with higher energy as expected¹ but is almost independent of mosaicity. The better resolutions at the outer detectors, especially at the $25'$ analyser, are due to the analyser illuminating one part of the detector tubes more than the other. Thereby the effective detector width decreases, which in turn improves the distance collimation. The outermost detectors will have much smaller intensities than the central and can be omitted to get comparable statistics and signal-to-noise in the different channels.

Even though coarser mosaicity will lower the peak reflectivity, it will increase the total count rate provided there are enough detectors. The same effect can be achieved replacing the detector tubes with a position-sensitive detector. However, in this work we concentrate on a detector setup of thin tubes.

IV. ADVANCED INSTRUMENT DESIGNS

In addition to the improved performance offered by the prismatic analyser, there are several other techniques to improve the performance of triple axis-type spectrometers, such as focussing and multiplexing. The prismatic analyser concept will be most useful if combined with any of these techniques.

A. Focussing analysers

An important component in distance collimation is the limited analyser width that unfortunately also limits the cov-

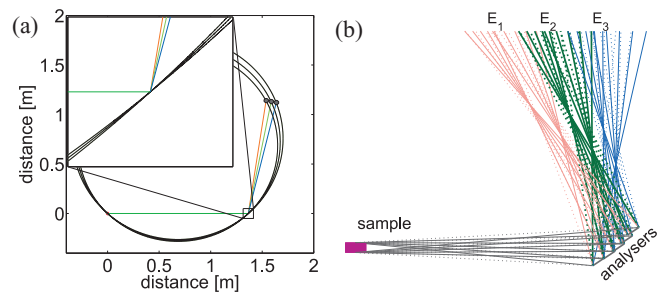


FIG. 4. (a) Illustration of the optimal Rowland Circles for three parallel $1/2''$ detector tubes. At the analyser positions the circles are very close together, making it possible to get almost perfect focussing for all three detectors from one focussing analyser. (b) The principle shown in Figure 2 for five analysers arranged in a Rowland geometry, the three energies, represented by different colors, are separated at the focussing distance.

ered solid angle. However, like in conventional analyser spectrometers, this can be countered by arranging the analysers in a focussing Rowland Geometry.¹⁵ The Rowland Geometry is robust to small perturbations in energy so the outer detectors will be in almost perfect focussing condition even when the analyser is focused on the central detector. Figure 4(a) displays the optimal Rowland circles for reflecting three different energies towards three different detectors from the same analyser position. At the analyser the distance between the circles is smaller than the width of the analyser crystals so the focussing is almost perfect for all detectors, independent of which of the circles is chosen. Figure 4(b) shows the schematics of how three different energies are reflected and how they can be separated at the detector position. The crystals are chosen to be so close that no gap is seen from the sample, but a small overlap between crystals is seen from the detector. Simulations have shown that this shadow effect is small when $L_{SA} \approx L_{AD}$ as it is in our example and for practical purposes the finite width of crystals and mounting will force the analysers further apart, eliminating the overlap.

By focussing it is possible to increase the solid angle coverage and thus improve the recorded flux just like with a conventional analyser setup. To confirm that it does indeed work we performed a full simulation with five analyser blades in a focussing geometry. This provided a factor 4.6 in flux gain without sacrificing energy resolution (data not shown).

B. Multiplexing

Multiplexing spectrometers have become increasingly popular with varying layouts like RITA II at PSI,^{16,17} and IMPS¹⁸ and Flatcone¹⁹ at ILL. A challenge when combining multiplexing with prismatic analysers is that many multiplexing instruments have several detectors close together measuring reflections from different analysers. There might thus not be sufficient space for the optimal number of detectors. However by choosing slightly sub-optimal settings it is still possible to combine the two techniques.

For example, the proposed ESS CAMEA will have a multiplexing setup with very large analyser coverage. It has 10 concentric rings of analysers reflecting 10 different prismatic energy bands, three of which are seen in Figure 5, to position

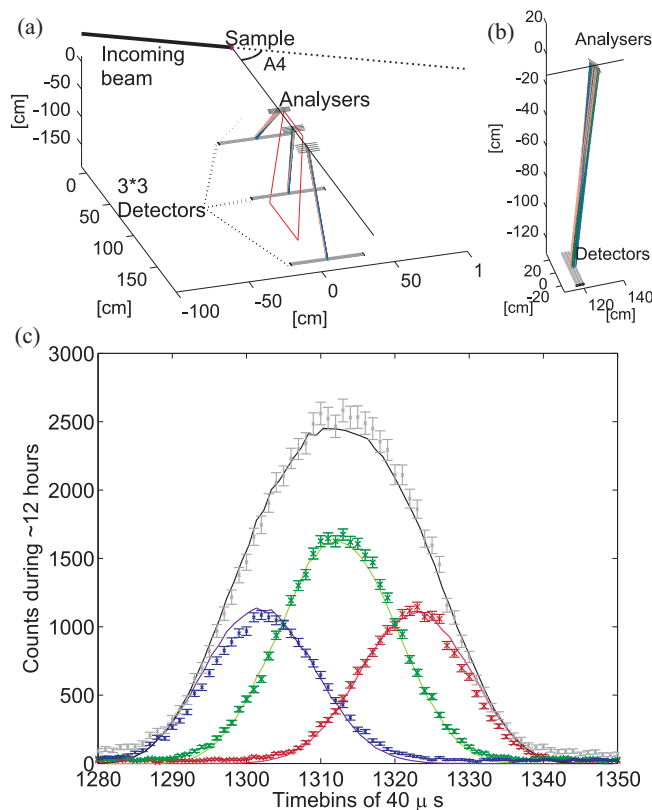


FIG. 5. (a) Sketch of the experimental setup of the CAMEA prototype. The analyser-detector setup in the red box is shown in (b). Data from this single analyser-detector setup are below. (c) Time distribution of neutrons scattered by a 2.2 cm tall cylindrical Vanadium sample with a radius of 5 mm and detected in each of the three detectors recording data from the 5 meV analyser. Measured data are given by data points and simulated data by solid lines. The colored peaks show the result of using the prismatic analyser while the gray shows the corresponding signal from adding all three detectors together and relying on 30' mosaicity for energy resolution. The simulated intensities have been rescaled by one common factor in order to compare the line shapes. The data are displayed in raw time bins. Each time bin of 40 μ s corresponds to an energy difference of ~ 10 μ eV.

sensitive detectors below the scattering plane.²⁰ While this extreme case of multiplexing could be combined with any number of detectors per analyser, a detector number above three would force the innermost analysers further apart than optimal and impose severe extra costs. In contrast, three detectors can be included without any drawbacks.²¹

V. EXPERIMENTAL VERIFICATION

A prototype of the ESS CAMEA prismatic analyser was built at the Technical University of Denmark and installed on the MARS backscattering spectrometer at PSI²² in 2012. MARS is an inverse time-of-flight instrument with a flight path between the master chopper and sample of 38.47 m. The prototype consists of 3 vertically focussing analysers behind each other. Each analyser consists of five 15 cm wide, 1 cm tall analysers placed above each other in Rowland geometry which scatter the neutrons out of the plane to 3 linear position-sensitive detectors tubes with a diameter of 0.5 in. The distance between sample and analyser is 1.2 m and between analyser and detectors 1.0 m. The analysers are cen-

tered around a 2θ value of 60° . Due to spatial restrictions in the prototype, the test was not performed at the exact settings proposed for the final CAMEA instrument. A more thorough description of the prototype and its testing will be reported in Ref. 23.

Figure 5 shows data obtained from the prototype experiment at the 5 meV analyser. In (c) we used a 2.2 cm tall Vanadium sample to ensure incoherent elastic scattering and recorded the energy separation expressed as neutron time-of-flight in the three detectors. The simulations were done at the same settings and the simulated intensities were rescaled with one common factor to account for imprecise descriptions of source brilliance, sample volume, and analyser peak reflectivity. The data are displayed in the raw time bins in order not to impose any data treatment assumptions. The data confirm that they are indeed possible to separate several energy bands and obtain the good resolution promised by the simulations from a focussing prismatic analyser in a multiplexing inverse time-of-flight spectrometer. The technique has also been tested at other distances and mosaicities and found to work equally well.

To test the prismatic analyser on a triple axis instrument, an experiment was performed on TASP,² PSI. TASP is a triple axis instrument with a vertically focussing monochromator, a horizontally focussing analyser with a mosaicity of 30' and a single ^3He detector tube with a width of $2' = 5.1$ cm. L_{SA} and L_{AD} were both set to 110 cm. The slits before and after the sample were left open and a Be filter inserted after the sample. The sample was a 4 cm high, 1 cm wide V rod, cooled to 10 K. Just before the detector, a slit was inserted to mimic the effect of a narrower detector and the detector arm was rotated to a number of different positions to represent several small detectors. For each position of the detector an E_i scan was performed around the analyser energy of $E_f = 4.6$ meV. The results for a 5 mm slit can be seen in Figure 6(a). The comparison of different settings can be seen in (c).

The 5 mm slit size corresponds to the point spread function of a typical position sensitive detector, while the 10 mm slit size is comparable to a thin (1/2 in./13 mm) detector tube. Both solutions provide considerably better resolution than the full detector. The similarity of the results from the 5 and 10 mm slit settings is due to the unmatched energy resolution, the largest contribution being from the monochromator. In this case, however, the unmatched resolution does not reduce the counts since all analysed neutrons are counted, although in different channels. However, the instrument becomes very sensitive to improved incoming energy resolution. In Fig. 6(b) the experiment from Fig. 6(a) was repeated without Be-filter and with the monochromator set at second order 10 meV (first order 2.5 meV) and the analyser at first order 10 meV. This rebalanced the resolutions, the incoming being relatively better. The data show a clear separation of the peaks from the different detectors.

For many experiments on TASP, a slit of variable size is inserted in front of the detector, leading to a smaller resolution improvement for the prismatic analyser. However, the prismatic system will record more neutrons and still have a better resolution than the single detector setup with any slit used at the same instrument.

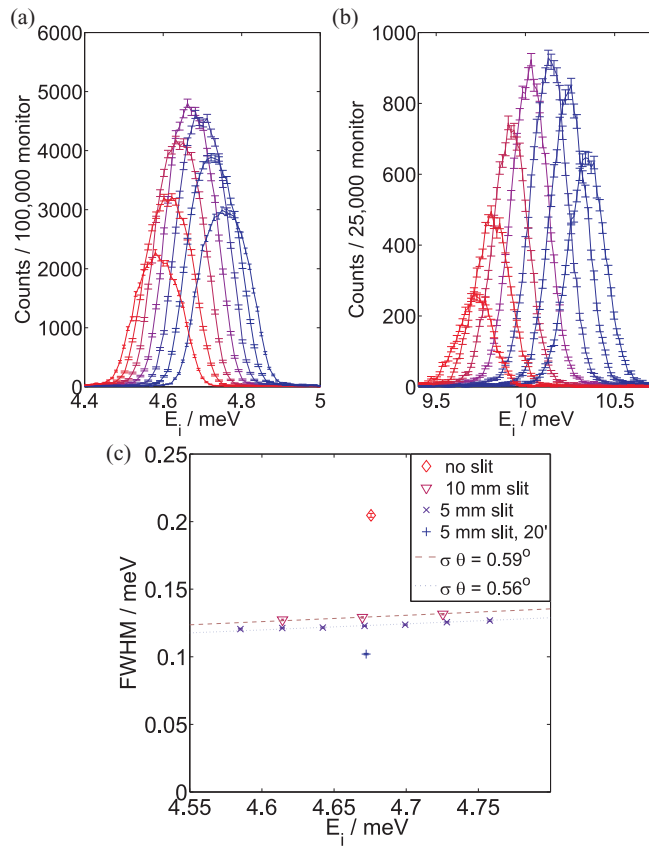


FIG. 6. (a) E_i scans of the elastic V line for 7 different detector positions on TASP with a 5 mm slit in front of the detector and a fixed analyser. (b) Using second order reflections from the monochromator and first order from the analyser it is possible to match the energy resolutions. (c) Comparison of elastic energy resolutions of TASP depending on slit size. The lines represent the standard resolution dependence on energy found by differentiating Bragg's law and fitting $\delta\theta$ to the data points. When a 20' collimator is inserted after the monochromator (blue cross) the resolution is improved further.

VI. COMPARISON TO A CONVENTIONAL SPECTROMETER

Table I shows examples of simulated gain factors for prismatic analysers. The resolution reduction is understood as $\sigma_r/\sigma_{\text{new}}$ where σ_{new} is determined from the central 5 meV detector and σ_r is the resolution of the reference setup. The intensity gain is defined as $(\sum_n I_n) \cdot R_\eta / (I_r \cdot R_{25'})$ where I_n is the intensity of the n th tube looking at a given analyser and I_r is the intensity on the reference detector. R_η is the peak re-

TABLE I. Gain factors for different prismatic analyser layouts obtained by simulations, using the standard geometry.

Analyser mosaicity	No. of detector tubes	Resolution reduction	Intensity gain
25'	3	2.0	0.9
60'	3	2.0	1.4
60'	5	2.0	1.9
90'	3	2.0	1.4
90'	5	2.0	2.0
90'	7	2.0	2.3

flectivity of the analyser with mosaicity η . The comparison is done for a vertical Rowland geometry as described in Sec. II, and for a reference using the same geometry but 25' analysers and a single detector taking up the same space as the full detector setup of the prismatic analyser. Hence the total width is 3.95 cm (including the 1 mm spacing between the detector tubes) when using three detectors and 6.65 cm wide when using five detectors. The Rowland geometry of the reference already gives a gain of 1.7 in flux and 1.7 in resolution reduction compared to a single 5 cm analyser. For this comparison we used typical peak reflectivity values of 0.8, 0.7, and 0.6 for 25', 60', and 90', respectively. The 0.9 in flux gain factor for three detectors and 25'' mosaicity is due to the difference between the three round detectors with less efficient edges and spacing between them and the single big square detector of the reference model.

The results demonstrate that it is possible to improve the resolution a factor of 2 while at the same time doubling the intensity compared to a traditional mosaicity driven analysers. This corresponds to a total gain factor of 4 if intensity and secondary energy resolution are assumed inversely proportional. Both gain factors can be increased slightly by using position sensitive detectors.

As discussed earlier there is only space for three detector tubes per analyser on CAMEA. Thus for this setting 60' mosaicity has been chosen for the design. This reduces the resolution a factor 2.0 and increases the flux a factor 1.4 for the ESS version when compared to a traditional Rowland geometry with the same analyser and detector area. Compared to a flat analyser slab one gains a factor of 3.3 in resolution reduction and 2.4 in flux or a total gain factor of 7.9. The same factor would be found if this analyser system was installed elsewhere, e.g., on a conventional TAS.

VII. CONCLUSION

We have showed that crystal analyser spectrometers designed for small samples can have a better distance collimation than the mosaicity of standard triple axis spectrometers. Instead of reducing the distance collimation or accept lower count rates the geometric constraints can be used as a benefit by installing several detectors that record different energies from the same analyser. If the mosaicity is relaxed, this can simultaneously produce better resolution and higher total count rates than achievable by installing finer mosaicity analyser crystals in standard geometry at the spectrometer or by using Soller collimators. The method is proven by both measurements and simulations to work together with analysers arranged in Rowland geometries and multiplexing setups. The method was developed for indirect time of flight but has also been proven feasible with a traditional TAS setup.

We have further exemplified that a 60' mosaicity setup with three detector channels can lead to a resolution improvement of a factor 2.0 together with a flux increase of a factor of up to 1.4 compared to a conventional 25' mosaicity analyser and single detector with analysers in Rowland geometry. Even bigger gain factors of 3.3 in resolution reduction and 2.4 in flux can be achieved when compared to a flat analyser slab.

ACKNOWLEDGMENTS

This project was funded by the Danish and Swiss in-kind contributions to ESS design-update phase. We thank Astrid Schneidewind for insightful comments to the manuscript.

- ¹G. Shirane, S. M. Shapiro, and J. M. Tranquada, *Neutron Scattering with a Triple-Axis Spectrometer* (Cambridge University Press, 2002).
- ²P. Böni and P. Keller, in *Proceedings of the 4th Summer School on Neutron Scattering*, 1996, Vol. 96-02, p. 35.
- ³PANDA, “Panda restrax file” (2014).
- ⁴See <http://www-llb.cea.fr/en/fr-en/spectros-llb.pdf> for Saclay.
- ⁵L. Harriger, see www.ncnr.nist.gov/instruments/spins/spins_details.html for SPINS.
- ⁶K. Lefmann, U. Filges, F. Treue, J. J. K. Kirkensgaard, B. Plesner, K. S. Hansen, and K. H. Klenø, *Nucl. Instrum. Methods A* **1634**, S1 (2011).
- ⁷S. Peggs, R. Kreier, C. Carlile, R. Miyamoto, A. Paahlsson, M. Trojer, and J. G. Weisend II, “ESS technical design report,” Technical Report ESS, 2013.
- ⁸K. Lefmann and K. Nielsen, *Neutron News* **10**, 20 (1999).
- ⁹P. K. Willendrup, E. Farhi, and K. Lefmann, *Physica B* **350**, E735 (2004).
- ¹⁰M. P. Nieh, Z. Yamani, N. Kucerka, and J. Katsaras, *J. Phys.: Conf. Ser.* **251**, 012061 (2010).
- ¹¹C. R. H. Bahl, P. Andersen, S. N. Klausen, and K. Lefmann, *Nucl. Instrum. Methods B* **226**, 667 (2004).
- ¹²M. Kenzelmann, A. Zheludev, S. Raymond, E. Ressouche, T. Masuda, P. Böni, K. Kakurai, I. Tsukada, K. Uchinokura, and R. Coldea, *Phys. Rev. B* **64**, 054422 (2001).
- ¹³A. Moore, M. Popovici, and A. Stoica, *Physica B* **276–278**, 858 (2000).
- ¹⁴M. Adiba, N. Habiba, M. El-Mesirya, and M. Fathallah, in *Energy and Environment Research, Proceedings of the 8th Conference on Nuclear and Particle Physics*, 2011, p. 81.
- ¹⁵M. Skoulatos, K. Habicht, and K. Lieutenant, *J. Phys.: Conf. Ser.* **340**, 012019 (2012).
- ¹⁶K. Lefmann, D. F. McMorrow, H. M. Rønnow, K. Nielsen, K. N. Clausen, B. Lake, and G. Aeppli, *Physica B* **283**, 343 (2000).
- ¹⁷K. Lefmann, C. Niedermayer, A. Abrahamsen, C. Bahl, N. Christensen, H. Jacobsen, T. Larsen, P. Häfger, U. Filges, and H. M. Rønnow, *Physica B* **385–386**, 1083 (2006).
- ¹⁸M. Jiménez-Ruiz and A. Hiess, *Physica B* **385–386**, 1086 (2006).
- ¹⁹M. Kempa, B. Janousova, J. Saroun, P. Flores, M. Boehm, F. Demmel, and J. Kulda, *Physica B* **385–386**, 1080 (2006).
- ²⁰P. G. Freeman, J. O. Birk, M. Marko, N. B. Christensen, J. Larsen, C. Niedermayer, J. Fanni, A. L. R. Hansen, K. Lefmann, and H. Rønnow, The European Physical Journal, EPJ Web of Conferences, QENS/WINS 2014 Proceedings.
- ²¹H. M. Rønnow, K. Lefmann, N. B. Christensen, C. Niedermayer, F. J. M. Markó, J. O. Birk, M. Brtelsen, J. Larsen, and P. G. Freeman, “ESS instrument construction proposal CAMEA,” Technical Report ESS, 2014.
- ²²P. L. Tregenna-Piggott, F. Juranyi, and P. Allenspach, *Neutron News* **19**(1), 20 (2008).
- ²³M. Markó, J. O. Birk, P. G. Freeman, K. Lefmann, C. Niedermayer, N. B. Christensen, F. Jurányi, A. L. R. Hansen, and H. M. Rønnow, “Building and testing of prototype for CAMEA spectrometer” (unpublished).